HHS Public Access

Author manuscript

Oncogene. Author manuscript; available in PMC 2015 October 09.

Published in final edited form as:

Oncogene. 2015 April 9; 34(15): 1938–1948. doi:10.1038/onc.2014.143.

Activation of mTOR Pathway in Myeloid-derived Suppressor Cells Stimulates Cancer Cell Proliferation and Metastasis in *lal−/−* Mice

Ting Zhao[1], **Hong Du**[1,2], **Xinchun Ding**[1], **Katlin Walls**[1], and **Cong Yan**[1,2,3]

[1]Department of Pathology and Laboratory Medicine, Indiana University School of Medicine, Indianapolis, IN 46202

[2]IU Simon Cancer Center, Indiana University School of Medicine, Indianapolis, IN 46202

[3]Center for Immunobiology, Indiana University School of Medicine, Indianapolis, IN 46202

Abstract

Inflammation critically contributes to cancer metastasis, in which myeloid-derived suppressor cells (MDSCs) are an important participant. Although MDSCs are known to suppress immune surveillance, their roles in directly stimulating cancer cell proliferation and metastasis currently remain unclear. Lysosomal acid lipase (LAL) deficiency causes systemic expansion and infiltration of MDSCs in multiple organs and subsequent inflammation. In the LAL-deficient ($lal^{-/-}$) mouse model, melanoma metastasized massively in allogeneic $lal^{-/-}$ mice, which was suppressed in allogeneic $lal^{+/+}$ mice due to immune rejection. Here we report for the first time that MDSCs from $lal^{-/-}$ mice directly stimulated B16 melanoma cell *in vitro* proliferation, and *in vivo* growth and metastasis. Cytokines i.e., IL-1β and TNFα from MDSCs are required for B16 melanoma cell proliferation *in vitro*. Myeloid-specific expression of human LAL (hLAL) in $lal^{-/-}$ mice rescues these malignant phenotypes *in vitro* and *in vivo*. The tumor-promoting function of $lal^{-/-}$ MDSCs is mediated, at least in part, through over-activation of the mammalian target of rapamycin (mTOR) pathway. Knockdown of mTOR, Raptor or Rictor in $lal^{-/-}$ MDSCs suppressed their stimulation on proliferation of cancer cells, including B16 melanoma, LLC and Tramp-C2 cancer cells. Our results indicate that LAL plays a critical role in regulating MDSCs ability to directly stimulate cancer cell proliferation, and overcome immune rejection of cancer metastasis in allogeneic mice through modulation of the mTOR pathway, which provides a mechanistic basis for targeting MDSCs to reduce the risk of cancer metastasis. Therefore, MDSCs possess dual functions to facilitate cancer metastasis: suppress immune surveillance, and stimulate cancer cell proliferation and growth.

Correspondence: Dr. Cong Yan, Department of Pathology and Laboratory Medicine, Indiana University School of Medicine, 975 W Walnut Street, IB424G, Indianapolis, IN 46202. coyan@iupui.edu; or Dr. Hong Du, Department of Pathology and Laboratory Medicine, Indiana University School of Medicine, 975 W Walnut Street, IB424E, Indianapolis, IN 46202. hongdu@iupui.edu.

Conflict of interest

The authors declare no conflict of interest.

Keywords

Lysosomal acid lipase; neutral lipid metabolism; myeloid-derived suppressor cells; mTOR; tumor growth and metastasis

Introduction

Inflammation plays crucial roles at all stages of tumor development, from tumor initiation to metastatic progression [1]. Metastasis, the leading cause of cancer-associated mortality, requires close collaboration between cancer cells and inflammatory cells [1]. Lysosomal acid lipase (LAL) hydrolyzes cholesteryl esters and triglycerides in the lysosome of cells to generate free fatty acids and cholesterol. Genetic ablation of the *lal* gene in mice has resulted in a systemic increase of myeloid lineage cells, causing severe inflammation in multiple organs [2, 3]. We have previously reported spontaneous lung adenocarcinoma in transgenic mice with myeloid-specific overexpression of matrix metalloproteinase 12 (MMP12) [4], or apoptosis inhibitor 6 (Api6/AIM/Spα) [5], or dominant negative peroxisome proliferators-activated receptor-γ (PPARγ) [6], all of which are downstream target or effector genes of LAL.

The neutral lipid metabolic pathway controlled by LAL plays a critical role in the development and homeostasis of myeloid-derived suppressor cells (MDSCs), and LAL deficiency led to the infiltration and accumulation of MDSCs in various organs of the mice [2, 3, 7]. LAL-deficient ($lal^{-/-}$) MDSCs arise from dysregulated production of progenitor cells in the bone marrow, and have strong suppressive function on T cells [2, 3, 7]. MDSCs, characterized by the co-expression of myeloid-cell lineage differentiation antigen Gr-1 and CD11b in mice, are a heterogeneous population of immature myeloid cells at different stages of differentiation [8]. In $lal^{-/-}$ mice, almost all Gr-1^+ cells are positive for CD11b [5]. Most $lal^{-/-}$ MDSCs stained double positive for Ly6G and Ly6C (collectively called Gr-1) [5]. Numerous studies have shown that an immunosuppressive state of MDSCs favors primary tumor development [9–15], but whether there is a direct stimulation of MDSCs on cancer cell proliferation and growth has not been confirmed. Therefore, the $lal^{-/-}$ animal model is a perfect system to address this issue. In humans, altered mononuclear phagocyte differentiation (increased $CD14^+CD16^+$ and $CD14^+CD33^+$ cells, subsets of human MDSCs) has been reported with heterozygote carriers of LAL mutations [16]. Patient with mutations in the LAL gene has been reported to be associated with carcinogenesis [17].

The mammalian target of rapamycin (mTOR) is a serine/threonine protein kinase that regulates cell growth, proliferation, migration, survival, protein synthesis, and transcription in response to growth factors and mitogens [18]. mTOR is the catalytic subunit of two distinctive complexes: mTOR complex 1 (mTORC1) and mTOR complex 2 (mTORC2). Unique accessory proteins, regulatory-associated protein of mTOR (RAPTOR), and rapamycin-insensitive companion of mTOR (RICTOR) define the TORC1 and TORC2 complexes, respectively [19]. Oncogenic activation of the mTOR pathway has been reported to induce several processes required for cancer cell growth, survival and proliferation [20]. However, its role in MDSCs is poorly understood. We have recently demonstrated that the

mTOR pathway is over-activated in bone marrow-derived *lal*$^{-/-}$ MDSCs [21]. It is entirely unknown whether the activation of the mTOR pathway in *lal*$^{-/-}$ MDSCs plays a role in tumor development and metastasis.

In the present study, we focused on the effects of *lal*$^{-/-}$ MDSCs on proliferation, growth and metastasis of cancer cells, especially B16 melanoma cells. Our study demonstrates for the first time that *lal*$^{-/-}$ MDSCs directly stimulate B16 melanoma cell proliferation, growth and metastasis by over-activation of the mTOR pathway in the allogeneic mouse model. These findings provide not only a mechanistic insight into the LAL deficiency in facilitating metastasis, but also a potential target on MDSCs for anti-tumor therapy.

Results

LAL deficiency stimulated B16 melanoma cell growth and metastasis

To see whether LAL deficiency-induced inflammation influences tumor progression and metastasis, the B16 melanoma cell model was used for subcutaneous and intravenous injection in allogeneic wild type (*lal*$^{+/+}$) and *lal*$^{-/-}$ FVBN mouse models. To examine growth potential *in vivo*, B16 melanoma cells were injected subcutaneously into mice. Large subcutaneous tumors were developed in 10 of 10 *lal*$^{-/-}$ mice, while only 1 of 10 *lal*$^{+/+}$ mice developed tumors. In addition, the tumors from *lal*$^{-/-}$ mice (tumor volume = 1189.8 ± 554.03mm^3) were significantly larger when compared with those developed in *lal*$^{+/+}$ mice (tumor volume = 48.0 ± 31.23mm^3, $p<0.0001$) at 3 weeks post-tumor cell injection (Figure 1a and b). Next, B16 melanoma cells were injected into the tail veins of mice to detect metastatic potential. Two weeks after injection, more B16 melanoma colonies were observed in *lal*$^{-/-}$ mice at the distal lung and liver organs (Figure 1c). Haematoxylin and eosin (H&E) staining revealed more neoplastic melanoma cells in the lungs of *lal*$^{-/-}$ mice than those of *lal*$^{+/+}$ mice (Figure 1d). Myeloid cell expansion is a major manifestation in *lal*$^{-/-}$ mice [2, 3]. To evaluate the effects of LAL in myeloid lineage cells on B16 melanoma cell metastasis, a doxycycline-inducible hLAL myeloid-specific expressing Tg/KO triple mouse model was used [3, 7]. Statistical analysis displayed that two weeks after intravenous injection of B16 melanoma cells, doxycycline-treated Tg/KO triple mice showed reduced number of melanoma colonies in the lungs compared with untreated mice (Figure 1e), suggesting that hLAL expression in *lal*$^{-/-}$ myeloid cells partially restored immune rejection of B16 melanoma cells in the allogeneic mice model. In tumor growth assessment, B16 melanoma cells were subcutaneously injected into the flank region of Tg/KO triple mice. Figure 1f showed that the volume of tumors from doxycycline-treated Tg/KO triple mice was decreased by 50% compared with those developed in untreated mice at 2 weeks post-injection. Taken together, LAL in myeloid lineage cells plays a critical role in rendering immune rejection of cancer cells in the allogeneic mouse model.

LAL deficiency in Ly6G$^+$ cells stimulated B16 melanoma cell proliferation

In *lal*$^{-/-}$ mice, systemic Ly6G$^+$CD11b$^+$ MDSCs elevation has been observed in multiple organs [2, 3, 7]. To evaluate the influence of *lal*$^{-/-}$ Ly6G$^+$CD11b$^+$ MDSCs on proliferation of B16 melanoma cells, freshly isolated bone marrow-derived *lal*$^{+/+}$ or *lal*$^{-/-}$ Ly6G$^+$ cells were co-cultured with B16 melanoma cells for 72 h. In *lal*$^{-/-}$ mice, since almost all Ly6G$^+$ cells

are positive for CD11b, Ly6G antibody was used for purification of $Ly6G^+CD11b^+$ cells [5]. As shown in Figure 2a, the number of B16 melanoma cells was significantly increased after co-culture with $lal^{-/-}$ $Ly6G^+$ cells, suggesting that $lal^{-/-}$ $Ly6G^+$ cells exert a directly stimulatory effect on proliferation of B16 melanoma cells *in vitro*. When $Ly6G^+$ cells from doxycycline-treated Tg/KO triple mice were co-cultured with B16 melanoma cells *in vitro*, reduced proliferation of B16 melanoma cells was observed, compared with those of untreated Tg/KO triple mice. Since *in vitro* co-culture conditions are not representative of the tumor microenvironment, *in vivo* co-culture experiment was performed to study the effect of $lal^{-/-}$ $Ly6G^+$ cells on B16 melanoma cell growth. Matrigel mixed with $lal^{+/+}$ or $lal^{-/-}$ $Ly6G^+$ cells and B16 melanoma cells were subcutaneously injected into allogeneic recipient $lal^{+/+}$ mice. Ten days later, the plugs mixed with $lal^{-/-}$ $Ly6G^+$ cells and B16 melanoma cells showed larger size than those mixed with $lal^{+/+}$ $Ly6G^+$ cells and B16 melanoma cells. Consistently, H&E staining revealed robust melanoma cell proliferation in the plugs containing $lal^{-/-}$ $Ly6G^+$ cells, while $Ly6G^+$ cells from doxycycline-treated Tg/KO triple mice decreased B16 melanoma cell growth (Figure 2b). Therefore, $lal^{-/-}$ MDSCs possess directly stimulatory activity on cancer cell proliferation.

Activated MDSCs secrete cytokines that contribute to tumor cell invasion, proliferation, and survival [22]. In $lal^{-/-}$ $Ly6G^+$ cells, mRNA levels of IL-1β and TNFα were up-regulated by a Real-time PCR analysis, while IL-6 showed no statistical difference (Figure 2c). To examine whether these cytokines secreted by $lal^{-/-}$ $Ly6G^+$ cells facilitate melanoma cell proliferation, transwell study was performed with $Ly6G^+$ cells seeding in the upper chamber and melanoma cells in the lower chamber. After 72 hours co-culture, the number of B16 melanoma cells that were co-cultured with $lal^{-/-}$ $Ly6G^+$ cells was significantly increased (Figure 2d). When $Ly6G^+$ cells were treated with anti-IL-6, IL-1β, or TNFα antibodies to neutralize cytokines, the stimulatory effects on melanoma cell proliferation were significantly inhibited in anti-TNFα antibody treated group. Although anti-IL-6 and anti-IL-1β antibodies showed no statistically significant effect, combination of all three cytokine antibodies further blocked the stimulatory effect of melanoma cell proliferation by $lal^{-/-}$ $Ly6G^+$ cells (Figure 2d). Therefore, cytokines (especially TNFα) secreted by $lal^{-/-}$ $Ly6G^+$ cells are, at least in part, responsible for mediating stimulatory effects on cancer cells.

LAL deficiency in $Ly6G^+$ cells facilitated B16 melanoma cell metastasis

Since $lal^{-/-}$ $Ly6G^+$ cells possess both immune suppressive function on T cells [3] and stimulatory function on cancer cells, it is intriguing to investigate if $lal^{-/-}$ $Ly6G^+$ cells facilitate B16 melanoma cell metastasis. Two weeks after intravenous co-injection, melanoma metastasized more aggressively in allogeneic recipient $lal^{+/+}$ mice with co-injection of $lal^{-/-}$ $Ly6G^+$ cells and B16 melanoma cells than those with $lal^{+/+}$ $Ly6G^+$ cells and B16 melanoma cells (Figure 3a and b). H&E staining and immunohistochemical (IHC) staining of the lung sections displayed more neoplastic melanoma cells and Ki67 positive proliferative cells in the lungs of $lal^{-/-}$ $Ly6G^+$ cell-injected recipient mice than those from $lal^{+/+}$ $Ly6G^+$ cell-injected recipient mice (Figure 3c).

mTOR inhibition impaired the ability of *lal*$^{-/-}$ Ly6G^{+} cells to enhance B16 melanoma cell proliferation and growth

We have recently reported that genes involved in the mTOR signaling pathway were altered in bone marrow-derived *lal*$^{-/-}$ Ly6G^{+} cells by Affymetrix GeneChip microarray [21]. This was confirmed by Western blot assay, in which mTOR downstream effectors p70S6K and S6 were highly phosphorylated in *lal*$^{-/-}$ Ly6G^{+} cells (Figure 4a), indicating over-activation of the mTOR pathway. To see whether over-activation of the mTOR pathway contributes to stimulation of *lal*$^{-/-}$ Ly6G^{+} cells on cancer cell proliferation, Ly6G^{+} cells were transfected with mTOR siRNAs. The knockdown efficiency of several mTOR siRNAs in myeloid cells was confirmed by the mTOR protein level and its downstream effectors in Western blot assay (Supplementary Figure 1). For the *in vitro* co-culture study, both *lal*$^{+/+}$ and *lal*$^{-/-}$ Ly6G^{+} cells with mTOR knockdown significantly reduced their abilities to stimulate proliferation of B16 melanoma cells (Figure 4b). Similar results were observed in *in vivo* co-culture Matrigel assay, which showed less neoplastic cells in the plugs with mTOR siRNA inhibition in *lal*$^{-/-}$ Ly6G^{+} cells (Figure 4c). This was supported by IHC staining, in which less Ki67 positive cells were monitored after mTOR knockdown in Ly6G^{+} cells (Figure 4d). In the tumor areas, positive cells for the endothelial marker CD31, the monocyte/macrophage marker F4/80, or T cell marker CD3 were all decreased following mTOR knockdown in Ly6G^{+} cells, especially knockdown in *lal*$^{-/-}$ ly6G^{+} cells, indicating that both tumor-associated angiogenesis and inflammatory cell infiltration were impaired (Figure 4d). Taken together, these results suggest that over-activation of the mTOR pathway plays a very important role in *lal*$^{-/-}$ Ly6G^{+} cells to stimulate B16 melanoma cell proliferation and growth.

mTOR Inhibition impaired the ability of *lal*$^{-/-}$ Ly6G^{+} cells to facilitate B16 melanoma cell metastasis

The role of mTOR pathway in *lal*$^{-/-}$ Ly6G^{+} cell-facilitated B16 melanoma cell metastasis was further examined. *lal*$^{+/+}$ or *lal*$^{-/-}$ Ly6G^{+} cells after mTOR siRNA transfection were co-injected with B16 melanoma cells into allogeneic recipient *lal*$^{+/+}$ mice intravenously. Two weeks later, mice injected with mTOR siRNA-transfected *lal*$^{-/-}$ Ly6G^{+} cells developed less melanoma metastatic lesions in their lungs (Figure 5a). Sections of the lungs showed less neoplastic cells by H&E staining (Figure 5b) and less Ki67 positive cells by IHC staining (Figure 5c). These observations suggest that over-activation of the mTOR signaling pathway in *lal*$^{-/-}$ Ly6G^{+} cells facilitates B16 melanoma cell metastasis.

Raptor and Rictor inhibition impaired the abililty of *lal*$^{-/-}$ Ly6G^{+} cells to enhance B16 melanoma cell proliferation, growth and metastasis

To assess which mTOR complexes (mTORC1 or mTORC2) is involved in *lal*$^{-/-}$ Ly6G^{+} cells' stimulatory effects, Ly6G^{+} cells were transfected with Raptor, Rictor or control siRNAs. The decreased protein expression levels of Raptor and Rictor in Ly6G^{+} cells after siRNAs transfections have been confirmed previously [19]. For *in vitro* co-culture study, Raptor and Rictor knockdown significantly reduced *lal*$^{-/-}$ Ly6G^{+} cell stimulation of melanoma cell proliferation (Figure 6a). Similarly, in the *in vivo* co-culture Matrigel assay, less neoplastic cells were detected in the plugs with Raptor and Rictor knockdown in *lal*$^{-/-}$

Ly6G$^+$ cells (Figure 6b). For *in vivo* metastasis study, less melanoma metastatic lesions developed in the lungs of mice that were co-injected with B16 melanoma cells and Raptor or Rictor siRNA-knockdown *lal*$^{-/-}$ Ly6G$^+$ cells, and H&E staining of lung sections showed significantly less neoplastic cells (Figure 6c). Taken together, both mTORC1 and mTORC2 are involved in *lal*$^{-/-}$ Ly6G$^+$ cell stimulation on B16 melanoma cell proliferation, growth and metastasis.

LAL deficiency in Ly6G$^+$ cells stimulated LLC and Tramp-C2 proliferation and growth, which was reversed by mTOR inhibition

To further confirm that *lal*$^{-/-}$ Ly6G$^+$ cells generally stimulate cancer cell proliferation and growth, the above experiments were repeated in two more cancer cell line models, LLC and Tramp-C2. In *in vitro* co-culture study, proliferation of LLC or Tramp-C2 was significantly increased after co-cultured with *lal*$^{-/-}$ Ly6G$^+$ cells (Figure 7a). As shown in Figure 7b and 7c, the Matrigel plugs mixed with *lal*$^{-/-}$ Ly6G$^+$ cells showed larger size and more Ki67 positive proliferative cells than those mixed with *lal*$^{+/+}$ Ly6G$^+$ cells. Furthermore, *lal*$^{-/-}$ Ly6G$^+$ cells with mTOR knockdown significantly reduced their abilities to stimulate cancer cell proliferation in *in vitro* co-culture experiment (Figure 7d). Therefore, *lal*$^{-/-}$ Ly6G$^+$ cells stimulate proliferation of multiple cancer cell models.

Discussion

LAL is a key enzyme in the metabolic pathway of neutral lipids. Based on extensive characterization, LAL has a tight connection with inflammation, and its deficiency results in multiple pathogenic phenotypes [2, 3, 7, 23, 24]. Strikingly, this report discovered that LAL deficiency-induced inflammation alleviated the immune rejection by allowing melanoma growth (Figure 1a and b) and metastasis to multiple organs in the allogeneic *lal*$^{-/-}$ mouse model (Figure 1c), suggesting that LAL is a critical lipid metabolic enzyme in tumor immunology. Understanding the cellular and molecular mechanisms underlying this observation will help identify potential targets for antitumor therapies.

The occurrence of metastasis requires cancer cells to survive in the circulation, arrive at the target organs, and show persistent proliferation and growth [25]. Such multistep process is inefficient in the allogeneic mouse model due to immune rejection. However, metastasis can be facilitated by the inflammatory environment, especially by interacting with inflammatory cells [1]. Since hLAL expression in *lal*$^{-/-}$ myeloid cells partially restored immune rejection of B16 melanoma cell in the allogeneic mice model (Figure 1e and f), the myeloid compartment must be crucial in controlling cancer cell growth and metastasis. One major manifestation during LAL deficiency is systemic MDSC expansion and dysfunction in multiple organs of the mice [2, 3, 23, 26, 27], which arises from dysregulated production of myeloid progenitor cells in the bone marrow [2]. In *lal*$^{-/-}$ mice, most MDSCs are Ly6G and Ly6C double positive, which showed strong suppression on T cell proliferation and function [3], similar to those observed in tumor-bearing mice [14, 28, 29]. Since B16 melanoma cells metastasized massively in the allogeneic *lal*$^{-/-}$ mouse model, other unidentified functions of *lal*$^{-/-}$ MDSCs have been further explored in addition to their well-known immunosuppressive function.

Indeed, when bone marrow-derived *lal*$^{-/-}$ MDSCs were co-cultured with B16 melanoma cells *in vitro*, a directly stimulatory effect of *lal*$^{-/-}$ MDSCs on cancer cell proliferation was observed (Figure 2a). This process was partially mediated by several inflammatory cytokines secreted by *lal*$^{-/-}$ MDSCs (Figure 2c and d). This was further supported by *in vivo* Matrigel assay when *lal*$^{-/-}$ MDSCs and B16 melanoma cells were co-injected into allogeneic recipient *lal*$^{+/+}$ mice, which showed more robust cancer cell growth *in vivo* (Figure 2b). To our knowledge, this is the first study demonstrating that MDSCs are able to directly stimulate cancer cell proliferation both *in vitro* and *in vivo*. Importantly, proliferation of other cancer cell lines (LLC and Tramp-C2) was also directly stimulated by *lal*$^{-/-}$ MDSCs *in vitro* and *in vivo* (Figure 7a–c). Therefore, MDSCs not only possess immunosuppressive function to clear a way for cancer growth and progression, but also stimulate cancer cell proliferation directly. In these processes, LAL in myeloid cells is critically involved in controlling the immunosuppressive function and cancer cell proliferation-stimulating function, because MDSCs isolated from hLAL myeloid specifically-expressed *lal*$^{-/-}$ mice showed reduced ability to suppress T cell proliferation and function [3], and impaired stimulation on cancer cell proliferation (Figure 2a and b). Moreover, after intravenous co-injection of B16 melanoma cells and *lal*$^{-/-}$ MDSCs into allogeneic recipient *lal*$^{+/+}$ mice, more melanoma developed in the lungs (Figure 3a–c). Therefore, there are at least two cellular mechanisms for *lal*$^{-/-}$ MDSCs to facilitate cancer cell metastasis: 1) stimulate cancer cell proliferation; and 2) suppress immune surveillance. It is import to recognize that MDSCs is not the only factor that contributes to cancer proliferation and immune suppression. As demonstrated in Figure 1e and f, restoring LAL expression in the myeloid cells partially reduced tumor growth and metastasis. Similarly, LAL is not the only factor controlling MDSCs malformation and malfunction. The rescue of LAL in myeloid cells of c-fms/hLAL/KO mice only partially corrects the abnormality of *lal*$^{-/-}$ MDSCs [3].

Given the importance of *lal*$^{-/-}$ MDSCs in cancer cell metastasis, it is important to identify the molecular mechanisms that mediate *lal*$^{-/-}$ MDSCs malfunction, especially their stimulation on cancer cell proliferation. Identification of such mechanisms and pathways will help find pharmacological intervention in immune therapy for cancer treatment. To achieve this goal, the intrinsic molecular defects in *lal*$^{-/-}$ MDSCs were identified by Affymetrix GeneChip microarray analysis. Ingenuity Pathway Analysis of gene transcripts revealed up-regulation of multiple genes in the mTOR signaling pathway in *lal*$^{-/-}$ MDSCs. The mTOR-associated cellular defects, including increased reactive oxygen species (ROS) production, elevated ATP synthesis, and reduced membrane potential, have been observed in *lal*$^{-/-}$ MDSCs as we reported previously [21]. So far, there is no study has been done to evaluate whether and how the mTOR pathway in MDSCs influences cancer immunology. In the present study, we confirmed that LAL deficiency induced over-activation of the mTOR pathway in MDSCs by activating the mTOR downstream genes (Figure 4a). Inhibition of mTOR in *lal*$^{-/-}$ MDSCs by siRNA transfection not only impaired their stimulatory effects on cancer cell proliferation in *in vitro* co-culturing assay (Figure 4b and 7d) and *in vivo* Matrigel assay (Figure 4c and d), but also significantly retarded their ability on B16 melanoma cell metastasis (Figure 5). Tumor-associated F4/80^{+} macrophages, CD3^{+} T cells and CD31^{+} endothelial cells in the B16 melanoma cell-injected Matrigel plugs were also

reduced after inhibition of mTOR in *lal*$^{-/-}$ MDSCs by siRNA transfection (Figure 4d), suggesting that over-activation of the mTOR pathway in *lal*$^{-/-}$ MDSCs is a major molecular mechanism underlying their stimulatory effects on cancer cell proliferation and metastasis. Furthermore, both mTORC1 and mTORC2 were involved in the *lal*$^{-/-}$ MDSCs' stimulatory activity on B16 melanoma cell proliferation, growth and metastasis (Figure 6). In addition to *lal*$^{-/-}$ MDSCs, inhibition of mTOR, Raptor and Rictor also showed effects in *lal*$^{+/+}$ MDSCs (Figure 2, 6 and 7). The mTOR signaling pathway is involved in regulating cell growth, proliferation, migration, survival, protein synthesis, and transcription in response to growth factors and mitogens. It is conceivable that inhibition of mTOR may also suppress the normal functions of mTOR in wild type cells. While it is important to suppress abnormal activities of MDSCs during cancer treatment, it is critical to control dosage use for patient care in the future. Nevertheless, it is still beneficial to treat cancer patients by eliminating MDSCs to decrease tumor growth and metastasis, since the mTOR shows over-activation in tumor MDSCs.

Recently, we have shown that inhibition of mTOR in *lal*$^{-/-}$ mice 1) reduced bone marrow myelopoiesis and systemic MDSC expansion; 2) reversed the increased cell proliferation, decreased apoptosis, increased ATP synthesis, and increased cell cycling of bone marrow-derived MDSCs; 3) corrected enhanced *lal*$^{-/-}$ MDSCs development from lineage negative progenitor cells; and 4) reversed the immune suppression on T cell proliferation and function that are associated with decreased ROS production, and recovery from impairment of mitochondrial membrane potential [19]. These results indicate a critical role of LAL-regulated mTOR signaling in the production and function of *lal*$^{-/-}$ MDSCs.

In conclusion, neutral lipid metabolism controlled by LAL critically regulates MDSCs ability to directly stimulate cancer cell proliferation, metastasis, and immune suppression through modulation of the mTOR pathway. The mTOR pathway may be served as a novel target to modulate the emergence of MDSCs to reduce the risk of cancer metastasis.

Materials and Methods

Animals and cell lines

lal$^{+/+}$ and *lal*$^{-/-}$ mice of the FVBN background were bred in house. c-fms-rtTA/$(TetO)_7$-CMV-hLAL; *lal*$^{-/-}$(Tg/KO) triple mice of the FVBN background is a previously generated triple transgenic mouse model with myeloid-specific doxycycline-inducible expression of wild-type human LAL (hLAL) in *lal*$^{-/-}$ mice under the control of the c-fms promoter [3, 7]. All scientific protocols involving the use of animals have been approved by the Institutional Animal Care and Use Committee of Indiana University School of Medicine and followed guidelines established by the Panel on Euthanasia of the American Veterinary Medical Association. Animals were housed under Institutional Animal Care and Use Committee-approved conditions in a secured animal facility at Indiana University School of Medicine.

The murine B16 melanoma cell line, Lewis lung carcinoma (LLC) cell line, and transgenic mouse prostate cancer (TRAMP-C2) cell line (purchased from ATCC) were cultured in DMEM supplemented with 10% FBS (Gibco).

Isolation of bone marrow-derived MDSCs

MDSCs were isolated as we previously described [6, 21]. Briefly, bone marrow cells were isolated from the femurs and tibias of mice. Cells were first incubated with biotin-conjugated anti-Ly6G antibody at 4°C for 15 min. After washed with PBS, cells were then incubated with anti-biotin microbeads at 4°C for another 15 min. Subsequently, cells were subjected to magnetic bead sorting according to the manufacturer's instructions (Miltenyi Biotec.).

In vitro co-culture of MDSCs and B16 melanoma cells

A pilot study has been performed to determine the best ratio between MDSCs and B16 melanoma cells. B16 melanoma cells were harvested, resuspended and adjusted to density at 5×10^4 cells/mL. Isolated MDSCs were used immediately and the cell density was adjusted to 5×10^6 cells/mL. One hundred microliter of MDSCs and 100 μL of B16 melanoma cells were mixed, and seeded into a well of 96-well plates in DMEM supplemented with 10% FBS. Seventy-two hours later, unattached MDSCs were removed by washing with PBS, and the number of attached B16 melanoma cells was counted. Morphologically, MDSCs are much smaller than B16 melanoma cells for exclusion.

In vivo Matrigel plug assay with MDSCs and B16 melanoma cells

This assay was performed according to an established method with minor modifications [30]. MDSCs and B16 melanoma cells were collected separately. A pilot study has been performed to determine the best ratio between MDSCs and B16 melanoma cells. After washed with PBS, 1×10^6 MDSCs and 1×10^5 B16 melanoma cells were mixed, centrifuged and resuspended in 40 μL PBS and mixed with 500 μL Matrigel Basement Membrane Matrix (BD Biosciences) containing 15 units of heparin (Sigma-Aldrich). The cell-Matrigel-mixture was then injected subcutaneously into the abdomen of 3-month old $lal^{+/+}$ mice. After 10 days, the mice were sacrificed and plugs were harvested from underneath the skin.

Mouse metastasis models

Four-month old $lal^{+/+}$ or $lal^{-/-}$ mice were inoculated with 1×10^5 B16 melanoma cells subcutaneously into the flank region and tumor size (length×width$^2\times\pi/6$) was monitored every week for 3 weeks. For intravenous injection of B16 melanoma cells, 5×10^5 B16 melanoma cells in 200 μL PBS were injected into 4-month old $lal^{+/+}$ or $lal^{-/-}$ mice via tail vein. A pilot study has been performed to determine the best ratio between MDSCs and B16 melanoma cells. For co-injection of MDSCs and B16 melanoma cells via tail vein, 2×10^6 MDSCs and 5×10^5 B16 melanoma cells were mixed and incubated at 37°C, 5% CO_2 for 30 min. After the incubation, cells were centrifuged, resuspended, and injected intravenously into 4-month old recipient $lal^{+/+}$ mice. Two weeks after the injection, the mice were sacrificed and the lungs were harvested for examination of metastasis.

Histology and immunohistochemical staining

The harvested plugs and lungs were fixed with 4% paraformaldehyde in PBS at 4°C for overnight. After fixation and embedding in paraffin, tissue sections were cut to 5 μm thick. H&E staining and immunohistochemical staining were performed by the Histological Core

Facility, Department of Pathology and Laboratory Medicine, Indiana University. The following antibodies were tested: Ki67, CD31, CD3, and F4/80. Tumor area quantitative analyses were performed by Metamorph 6.02 (Molecular Devises) on images taken by Olympus microscopy image system.

Western blot analysis

Western blot analysis was performed as previously described [31]. Briefly, MDSCs were lysed in Cell Lytic MT lysis buffer (Sigma) with Protease Inhibitor Cocktail (Invitrogen) and phosphatase inhibitor 2 and 3 (Sigma) for 15 min on a shaker. After centrifugation for 20 min at 12 000×g (4°C), the supernatants were saved and protein concentrations of the samples were determined using the Pierce BCA Protein Assay Kit (Thermo Scientific). Equal amounts of protein (30 μg) were loaded onto SDS-polyacrylamide gels and blotted onto PVDF membranes (BioRad). Western blot analysis was performed using antibodies against mTOR, phospho-mTOR, p70S6K, phospho-p70S6K, S6, and phospho-S6 (rabbit monoclonal antibodies, 1: 1 000, Cell Signaling). Antibody against β-actin (rabbit monoclonal anti-β-actin, 1: 2 000, Cell Signaling) was used as a loading control. For detection, the membrane was incubated with anti-rabbit IgG secondary antibodies conjugated with horseradish peroxidase (1: 2 000, Cell Signaling). Bands were visualized using SuperSignal West Pico Chemiluminescent substrate (ThermoScientific Pierce).

Small interfering RNA transfection

Before transfection, MDSCs were seeded into 96-well plates at a density of 1×10^6 cells/well. For small interfering RNA (siRNA)-mediated gene knockdown, 50 nmol/L of mTOR siRNA SMARTpool (containing a mixture of several siRNAs targeting mTOR), Raptor siRNA, Rictor siRNA or control siRNA (Dharmacon) was transfected into MDSCs with DharmaFECT Transfection Reagent I (Dharmacon) according to the manufacturer's protocol. After 24 h of transfection, cells were harvested for further analysis.

Real-time RT-PCR

Total RNAs from $Ly6G^+$ cells were purified using the Qiagen total RNA purification kit (Qiagen). Quantitative (q)RT-PCR was performed as described previously [6]. Analysis was performed by the $2^{-\Delta\Delta CT}$ method. Primers of mIL-6, mIL-1β, mTNF-α and GAPDH for real-time PCR were described previously [6].

Transwell assay

For transwell experiment, 0.4-μm pore 6.5-mm diameter transwells were used to separate $Ly6G^+$ cells and B16 melanoma cells (Corning) to observe the effect of $Ly6G^+$ cell-secreted cytokines on melanoma cell proliferation. Freshly isolated 2×10^6 $Ly6G^+$ cells in 200 μL media were seeded into the upper chamber of transwells, while 2×10^4 melanoma cells in 600 μL media were placed in the lower chamber. For the neutralization study, $Ly6G^+$ cells were treated with 10 μg/mL neutralizing antibody against IL-6, IL-1β, TNF-α or control IgG. After 72 hours' culture, the transwells were removed, and the number of B16 melanoma cells in the lower chamber was counted.

Statistics

Data were expressed as mean ± SD. Differences between two treatment groups were compared by Student's *t*-test. When more than two groups were compared, one-way ANOVA with post-hoc Newman-Keul's multiple comparison test was used. Results were considered statistically significant when $P < 0.05$. All analyses were performed with GraphPad Prism 5.0 (GraphPad).

Supplementary Material

Refer to Web version on PubMed Central for supplementary material.

Acknowledgments

Grant support: This work was supported by National Institutes of Health Grants CA138759, CA152099 (to C. Y.) and HL087001 (to H. D.).

References

1. Grivennikov SI, Greten FR, Karin M. Immunity, Inflammation, and Cancer. Cell. 2010; 140:883–899. [PubMed: 20303878]
2. Qu P, Shelley WC, Yoder MC, Wu L, Du H, Yan C. Critical roles of lysosomal acid lipase in myelopoiesis. Am J Pathol. 2010; 176:2394–2404. [PubMed: 20348241]
3. Qu P, Yan C, Blum JS, Kapur R, Du H. Myeloid-specific expression of human lysosomal acid lipase corrects malformation and malfunction of myeloid-derived suppressor cells in lal−/− mice. J Immunol. 2011; 187:3854–3866. [PubMed: 21900179]
4. Qu P, Yan C, Du H. Matrix metalloproteinase 12 overexpression in myeloid lineage cells plays a key role in modulating myelopoiesis, immune suppression, and lung tumorigenesis. Blood. 2011; 117:4476–4489. [PubMed: 21378275]
5. Qu P, Du H, Li Y, Yan C. Myeloid-specific expression of Api6/AIM/Sp alpha induces systemic inflammation and adenocarcinoma in the lung. J Immunol. 2009; 182:1648–1659. [PubMed: 19155514]
6. Wu L, Yan C, Czader M, Foreman O, Blum JS, Kapur R, et al. Inhibition of PPARgamma in myeloid-lineage cells induces systemic inflammation, immunosuppression, and tumorigenesis. Blood. 2012; 119:115–126. [PubMed: 22053106]
7. Yan C, Lian X, Li Y, Dai Y, White A, Qin Y, et al. Macrophage-specific expression of human lysosomal acid lipase corrects inflammation and pathogenic phenotypes in lal−/− mice. Am J Pathol. 2006; 169:916–926. [PubMed: 16936266]
8. Gabrilovich DI, Nagaraj S. Myeloid-derived suppressor cells as regulators of the immune system. Nature reviews Immunology. 2009; 9:162–174.
9. Mandruzzato S, Solito S, Falisi E, Francescato S, Chiarion-Sileni V, Mocellin S, et al. IL4Rα+ Myeloid-Derived Suppressor Cell Expansion in Cancer Patients. The Journal of Immunology. 2009; 182:6562–6568. [PubMed: 19414811]
10. Diaz-Montero CM, Salem M, Nishimura M, Garrett-Mayer E, Cole D, Montero A. Increased circulating myeloid-derived suppressor cells correlate with clinical cancer stage, metastatic tumor burden, and doxorubicin–cyclophosphamide chemotherapy. Cancer Immunol Immunother. 2009; 58:49–59. [PubMed: 18446337]
11. Ko JS, Zea AH, Rini BI, Ireland JL, Elson P, Cohen P, et al. Sunitinib Mediates Reversal of Myeloid-Derived Suppressor Cell Accumulation in Renal Cell Carcinoma Patients. Clinical Cancer Research. 2009; 15:2148–2157. [PubMed: 19276286]
12. Hoechst B, Voigtlaender T, Ormandy L, Gamrekelashvili J, Zhao F, Wedemeyer H, et al. Myeloid derived suppressor cells inhibit natural killer cells in patients with hepatocellular carcinoma via the NKp30 receptor. Hepatology. 2009; 50:799–807. [PubMed: 19551844]

13. Wang L, Chang EWY, Wong SC, Ong S-M, Chong DQY, Ling KL. Increased Myeloid-Derived Suppressor Cells in Gastric Cancer Correlate with Cancer Stage and Plasma S100A8/A9 Proinflammatory Proteins. The Journal of Immunology. 2013; 190:794–804. [PubMed: 23248262]
14. Ostrand-Rosenberg S, Sinha P. Myeloid-derived suppressor cells: linking inflammation and cancer. J Immunol. 2009; 182:4499–4506. [PubMed: 19342621]
15. Bruchard M, Mignot G, Derangere V, Chalmin F, Chevriaux A, Vegran F, et al. Chemotherapy-triggered cathepsin B release in myeloid-derived suppressor cells activates the Nlrp3 inflammasome and promotes tumor growth. Nat Med. 2013; 19:57–64. [PubMed: 23202296]
16. Rothe G, Stohr J, Fehringer P, Gasche C, Schmitz G. Altered mononuclear phagocyte differentiation associated with genetic defects of the lysosomal acid lipase. Atherosclerosis. 1997; 130:215–221. [PubMed: 9126667]
17. Elleder M, Chlumska A, Hyanek J, Poupetova H, Ledvinova J, Maas S, et al. Subclinical course of cholesteryl ester storage disease in an adult with hypercholesterolemia, accelerated atherosclerosis, and liver cancer. J Hepatol. 2000; 32:528–534. [PubMed: 10735626]
18. Guertin DA, Sabatini DM. Defining the role of mTOR in cancer. Cancer Cell. 2007; 12:9–22. [PubMed: 17613433]
19. Ding X, Du H, Yoder MC, Yan C. Critical Role of the mTOR Pathway in Development and Function of Myeloid-Derived Suppressor Cells in lal(−/−) Mice. Am J Pathol. 2014; 184:397–408. [PubMed: 24287405]
20. Laplante M, Sabatini David M. mTOR Signaling in Growth Control and Disease. Cell. 2012; 149:274–293. [PubMed: 22500797]
21. Yan C, Ding X, Dasgupta N, Wu L, Du H. Gene profile of myeloid-derived suppressive cells from the bone marrow of lysosomal acid lipase knock-out mice. PLoS One. 2012; 7:e30701. [PubMed: 22383970]
22. Talmadge JE, Gabrilovich DI. History of myeloid-derived suppressor cells. Nature reviews Cancer. 2013; 13:739–752.
23. Lian X, Yan C, Yang L, Xu Y, Du H. Lysosomal acid lipase deficiency causes respiratory inflammation and destruction in the lung. Am J Physiol Lung Cell Mol Physiol. 2004; 286:L801–807. [PubMed: 14644759]
24. Qu P, Roberts J, Li Y, Albrecht M, Cummings OW, Eble JN, et al. Stat3 downstream genes serve as biomarkers in human lung carcinomas and chronic obstructive pulmonary disease. Lung Cancer. 2009; 63:341–347. [PubMed: 18614255]
25. Chambers AF, Groom AC, MacDonald IC. Metastasis: Dissemination and growth of cancer cells in metastatic sites. Nat Rev Cancer. 2002; 2:563–572. [PubMed: 12154349]
26. Lian X, Yan C, Qin Y, Knox L, Li T, Du H. Neutral lipids and peroxisome proliferator-activated receptor-{gamma} control pulmonary gene expression and inflammation-triggered pathogenesis in lysosomal acid lipase knockout mice. Am J Pathol. 2005; 167:813–821. [PubMed: 16127159]
27. Du H, Heur M, Duanmu M, Grabowski GA, Hui DY, Witte DP, et al. Lysosomal acid lipase-deficient mice: depletion of white and brown fat, severe hepatosplenomegaly, and shortened life span. J Lipid Res. 2001; 42:489–500. [PubMed: 11290820]
28. Joyce JA, Pollard JW. Microenvironmental regulation of metastasis. Nat Rev Cancer. 2009; 9:239–252. [PubMed: 19279573]
29. Meyer C, Sevko A, Ramacher M, Bazhin AV, Falk CS, Osen W, et al. Chronic inflammation promotes myeloid-derived suppressor cell activation blocking antitumor immunity in transgenic mouse melanoma model. Proceedings of the National Academy of Sciences. 2011; 108:17111–17116.
30. Bonauer A, Carmona G, Iwasaki M, Mione M, Koyanagi M, Fischer A, et al. MicroRNA-92a Controls Angiogenesis and Functional Recovery of Ischemic Tissues in Mice. Science. 2009; 324:1710–1713. [PubMed: 19460962]
31. Zhao T, Li J, Chen AF. MicroRNA-34a induces endothelial progenitor cell senescence and impedes its angiogenesis via suppressing silent information regulator 1. Am J Physiol Endocrinol Metab. 2010; 299:E110–116. [PubMed: 20424141]

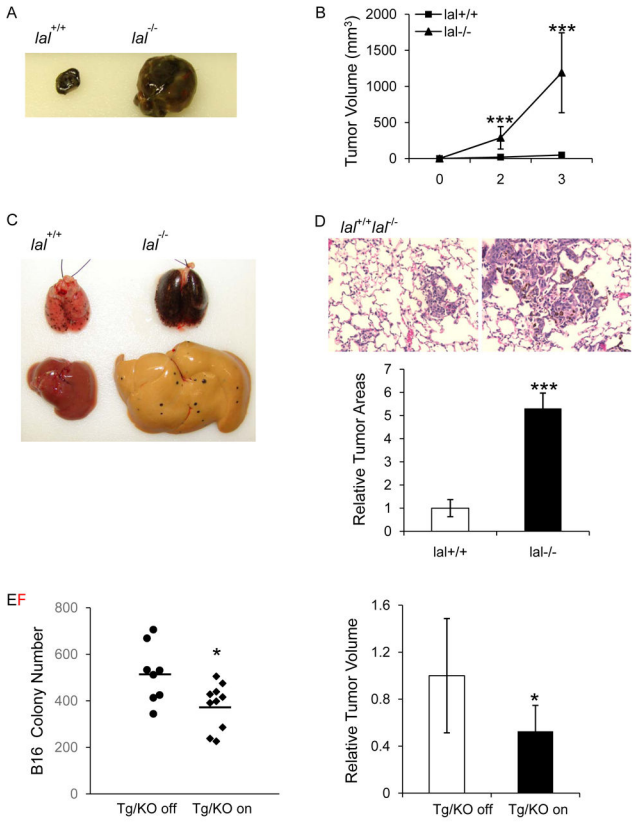

Figure 1. B16 melanoma cell growth and metastasis in *lal*$^{-/-}$ mice

(A) B16 melanoma cells (1×10^5) were subcutaneously injected into *lal*$^{+/+}$ or *lal*$^{-/-}$ mice for 3 weeks. A representative picture of tumor was shown. (B) Statistical analysis of tumor volume (in cubic millimeters). Data were expressed as mean ± SD; n = 10. ***P<0.0001 at week 2 and 3. (C) B16 melanoma cells (5×10^5) was intravenously injected into *lal*$^{+/+}$ or *lal*$^{-/-}$ mice for 2 weeks. Metastasized B16 melanoma colonies in the lungs and livers are shown. (n=10) (D) Representative H&E staining of lung sections and statistical analysis of relative tumor areas. Original magnification, ×200. Data were expressed as mean ± SD; n = 10. ***P<0.0001. (E) Quantitative analysis of B16 melanoma colonies in the lungs of doxycycline-treated or untreated Tg/KO triple mice with intravenous injection of 5×10^5 B16 melanoma cells for two week. n = 8~10. *P < 0.05. (F) Statistical analysis of relative tumor volume after B16 melanoma cells (1×10^5) were subcutaneously injected into doxycycline-treated or untreated Tg/KO triple mice for 2 weeks. Data were expressed as mean ± SD; n = 8. *P<0.05.

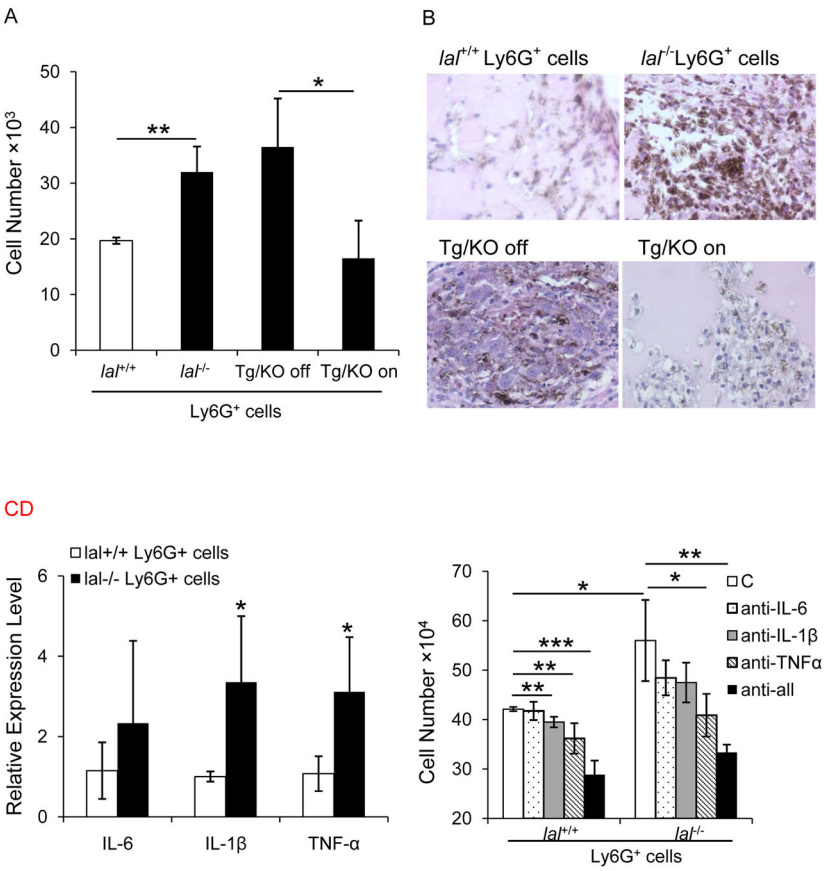

Figure 2. *lal*$^{-/-}$ Ly6G^{+} cells directly stimulated B16 melanoma cell proliferation and growth

(A) B16 melanoma cells (5× 10^3) were co-cultured with Ly6G^{+} cells (5× 10^5) from *lal*$^{+/+}$ or *lal*$^{-/-}$ mice, or doxycycline-treated or untreated Tg/KO triple mice *in vitro* for 72 h, and numbers of B16 melanoma cells were counted. Data were expressed as mean ± SD; n = 3~4. **P < 0.01, *P < 0.05. (B) Matrigel mixed with B16 melanoma cells (1× 10^5) and Ly6G^{+} cells (1× 10^6) was implanted subcutaneously into *lal*$^{+/+}$ mice for 10 days. Representative H&E staining of Matrigel plug sections is shown. Original magnification, ×400. (n=10 for Ly6G^{+} cells from *lal*$^{+/+}$ or *lal*$^{-/-}$ mice, and n=4 for Ly6G^{+} cells from doxycycline-treated or untreated Tg/KO triple mice). (C) Real-time PCR analysis of mRNA expression levels of cytokines in *lal*$^{-/-}$ vs. *lal*$^{+/+}$ Ly6G^{+} cells. The relative gene expression was normalized to GAPDH mRNA, and analysis was performed by the $2^{-\Delta\Delta CT}$ method. Data were expressed as means ± SD; n = 4. *P < 0.05. (D) To block cytokines, Ly6G^{+} cells (2×10^6) in 200 μL media were seeded into the upper chamber of 0.4-μm pore 6.5-mm diameter transwells, while B16 melanoma cells (2×10^4) in 600 μL media were placed in the lower chamber. For the neutralization study, Ly6G^{+} cells were treated with 10 μg/mL neutralizing antibody against IL-6, IL-1β, TNF-α individually or in combination, or control IgG. After 72 h, the number of B16 melanoma cells was counted. Data were expressed as mean ± SD; n = 4. ***P < 0.001, **P < 0.01, *P < 0.05.

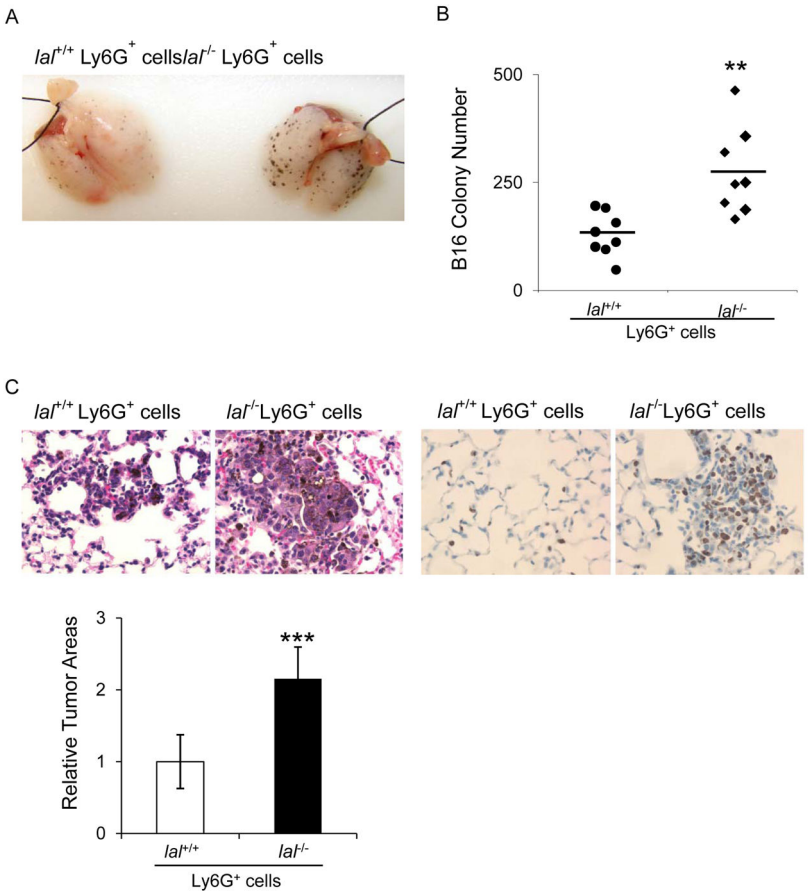

Figure 3. *lal*$^{-/-}$ Ly6G^{+} cells facilitated B16 melanoma cell migration and metastasis

(A) B16 melanoma cells (5× 10^5) and Ly6G^{+} cells (2× 10^6) from *lal*$^{+/+}$ or *lal*$^{-/-}$ mice were intravenously injected into *lal*$^{+/+}$ mice for 2 weeks. Representative lungs are shown. n = 10. (B) Quantitative analysis of the melanoma colony numbers in the lungs. Data were expressed as mean ± SD; n = 8. **P < 0.01. (C) Representative H&E staining and IHC staining with Ki67 antibody of the metastasized lungs is shown, including statistical analysis of relative tumor areas. Original magnification, ×400. Data were expressed as mean ± SD; n = 10. ***P<0.0001.

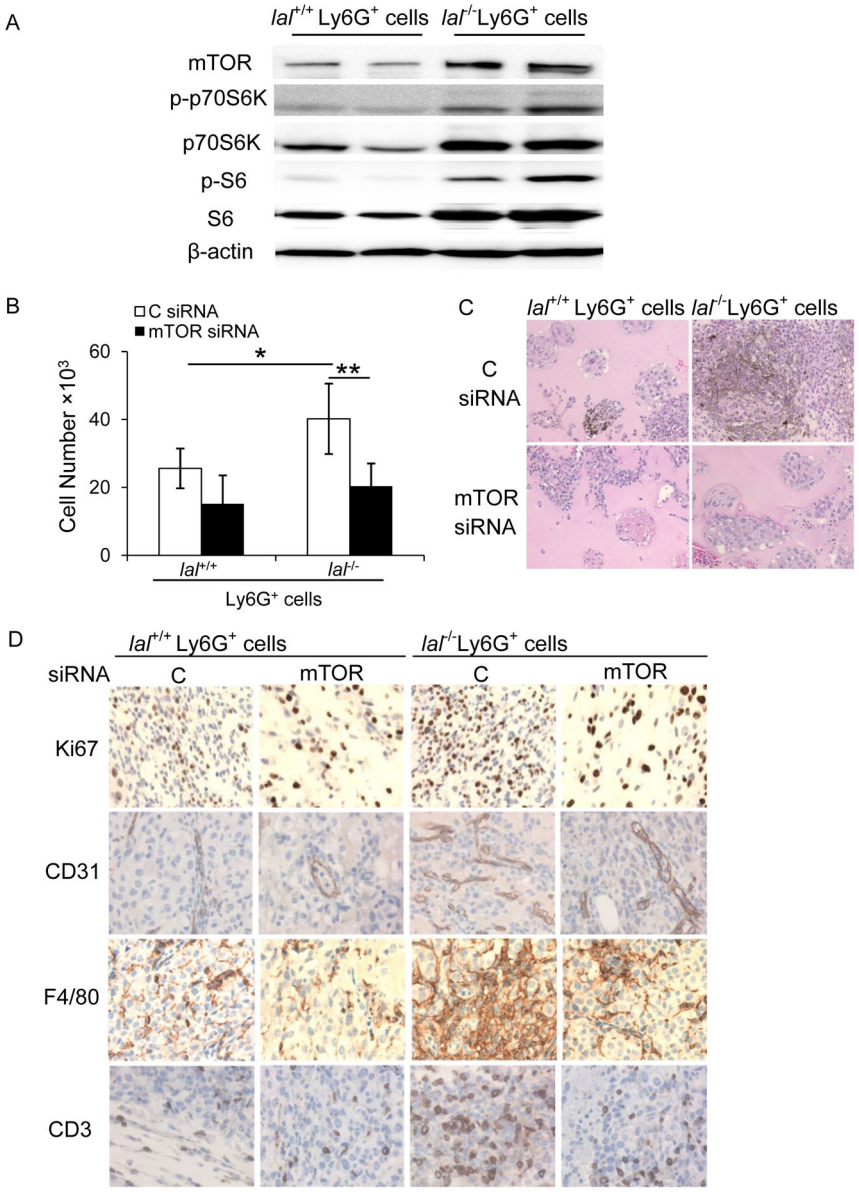

Figure 4. mTOR inhibition impaired the ability of *lal*$^{-/-}$ Ly6G^{+} cells to enhance B16 melanoma cell proliferation and growth

(A) Western blot analysis of the mTOR downstream proteins in *lal*$^{+/+}$ or *lal*$^{-/-}$ Ly6G^{+} cells. Representative blots were shown. (n=4). (B) Ly6G^{+} cells were transfected with mTOR siRNA SMARTpool (containing a mixture of siRNAs targeting mTOR) or control (C) siRNA for 24 h, and 5× 10^5 cells were co-cultured with B16 melanoma cells (5× 10^3) *in vitro*. The numbers of B16 melanoma cells were counted post 72 h. Data were expressed as mean ± SD; n = 5. *P < 0.05, **P < 0.01. (C) Ly6G^{+} cells (1× 10^6) after transfection were mixed with B16 melanoma cells (1× 10^5) in Matrigel and implanted subcutaneously into *lal*$^{+/+}$ mice for 10 days. Representative H&E staining of Matrigel plug sections is shown. Original magnification, ×200. (n=10) (D) Representative IHC staining of the Matrigel plug

sections using antibodies against Ki67, CD31, F4/80, and CD3. Original magnification, ×400.

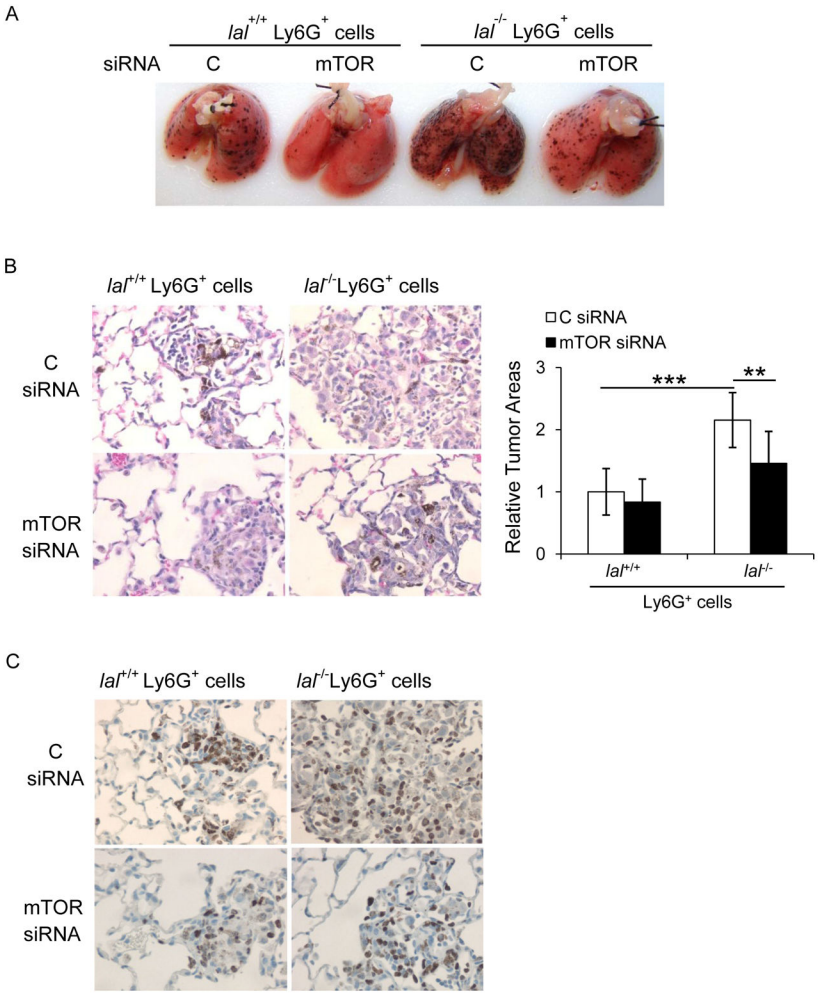

Figure 5. mTOR inhibition impaired the ability of *lal*$^{-/-}$ Ly6G^{+} cells to facilitate B16 melanoma cell metastasis

(A) Ly6G^{+} cells (2× 10^{6}) after siRNA transfection were co-injected with B16 melanoma cells (5× 10^{5}) into *lal*$^{+/+}$ mice via tail vein for 2 weeks. Representative lungs were shown. (n=5) (B) Representative H&E staining of metastasized lungs and statistical analysis of relative tumor areas. Original magnification, ×400. Data were expressed as mean ± SD; n = 5. ***P<0.001, **P<0.01. (C) Representative IHC staining of metastasized lungs using anti-Ki67-antibody was shown. Original magnification, ×400.

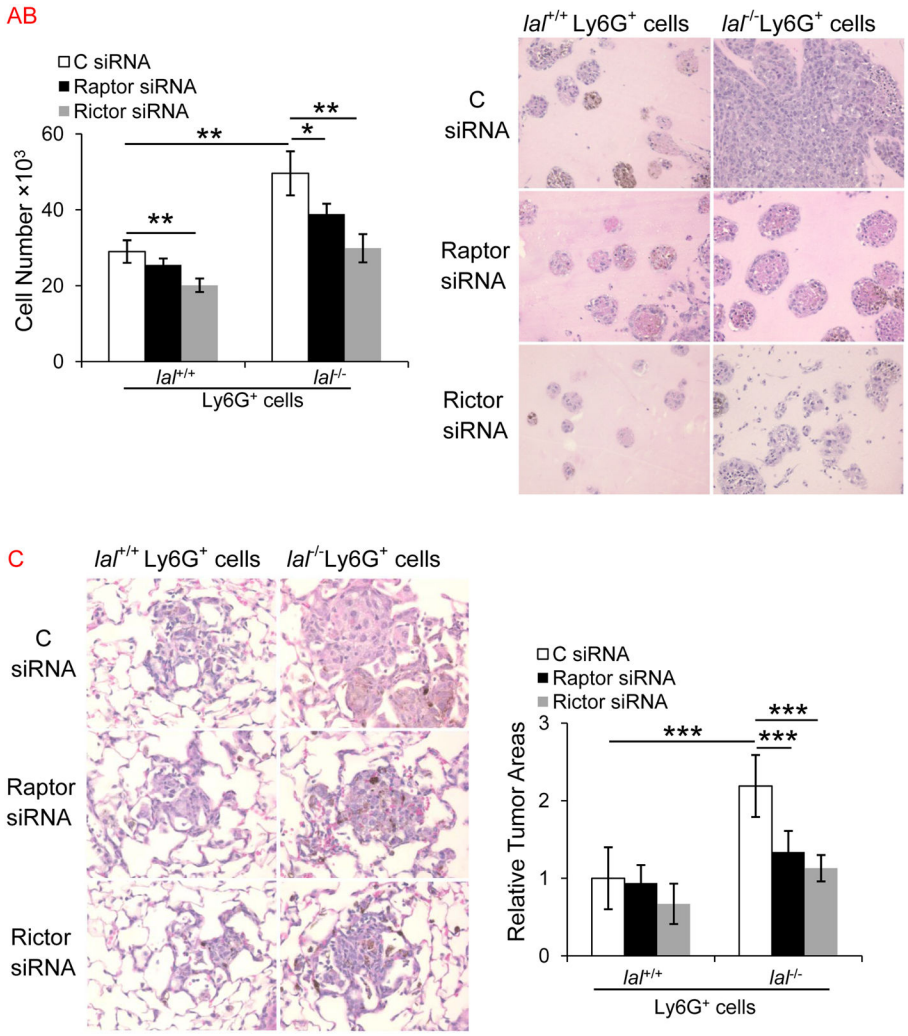

Figure 6. Raptor or Rictor inhibition impaired the ability of *lal*$^{-/-}$ Ly6G^{+} cells to enhance B16 melanoma cell proliferation, growth and metastasis

(A) Ly6G^{+} cells were transfected with Raptor, Rictor siRNA SMARTpool (containing a mixture of siRNAs targeting Raptor or Rictor) or control (C) siRNA for 24 h, and then co-cultured with B16 melanoma cells *in vitro*. The numbers of B16 melanoma cells were counted post 72 h. Data were expressed as mean ± SD; n = 4. *P < 0.05, **P < 0.01. (B) Ly6G^{+} cells after transfection were mixed with B16 melanoma cells in Matrigel and implanted subcutaneously into *lal*$^{+/+}$ mice for 10 days. Representative H&E staining of Matrigel plug sections is shown. Original magnification, ×200. (n=6) (C) Ly6G^{+} cells after transfection were co-injected with B16 melanoma cells intravenously into *lal*$^{+/+}$ mice for 2 weeks. Representative H&E staining of metastasized lungs and statistical analysis of relative tumor areas were shown. Original magnification, ×400. Data were expressed as mean ± SD; n = 7~8. ***P<0.001.

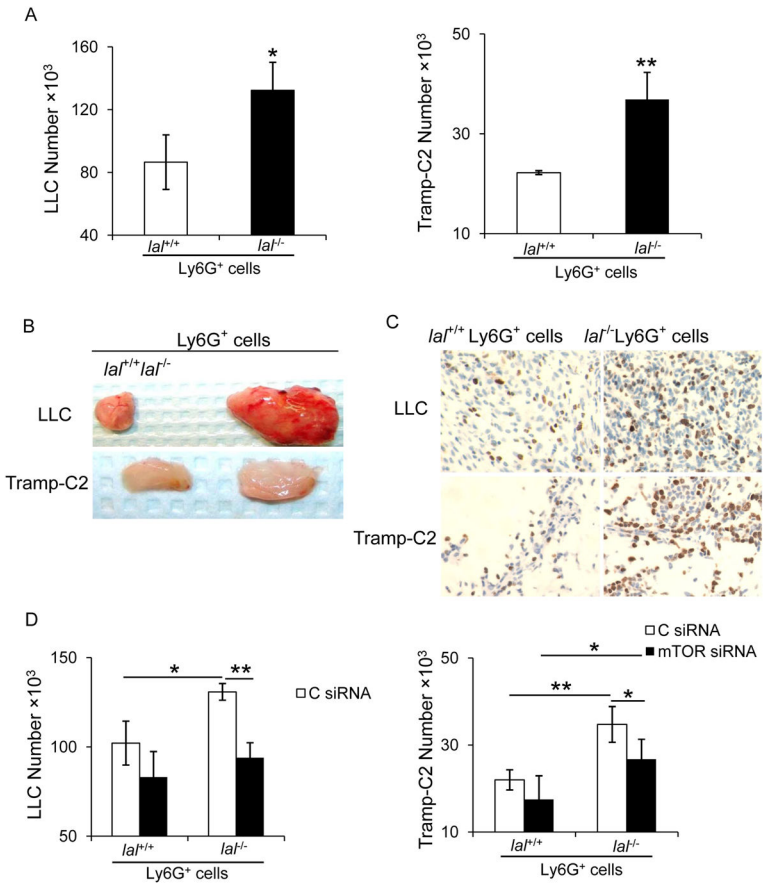

Figure 7. *lal*$^{-/-}$ Ly6G^{+} cells stimulated LLC and Tramp-C2 growth through over-activation of mTOR signaling pathway

(A) LLC cells or Tramp-C2 cells (1× 10^4) were co-cultured *in vitro* with *lal*$^{+/+}$ or *lal*$^{-/-}$ Ly6G^{+} cells (5× 10^5) for 72 h, and the numbers of LLC or Tramp-C2 cells were counted. Data were expressed as mean ± SD; n = 4. *P < 0.05, **P < 0.01. (B) LLC or Tramp-C2 cells (1× 10^5) and Ly6G^{+} cells (1× 10^6) were mixed in Matrigel and implanted subcutaneously into *lal*$^{+/+}$ mice for 10 days. Representative pictures of Matrigel plugs were shown. (n=4) (C) Representative IHC staining with anti-Ki67 antibody of Matrigel plug sections was shown. Original magnification, ×400. (D) Ly6G^{+} cells were transfected with mTOR siRNA or control (C) siRNA for 24 h, followed by co-culture with cancer cells *in vitro*. The numbers of LLC or Tramp-C2 cells were counted post 72 h. Data were expressed as mean ± SD; n = 4. *P < 0.05, **P < 0.01.